Designing an optimal PID controller for a PV-connected Zeta converter using genetic algorithm

Abadal-Salam T. Hussain[1], Faris Hassan Taha[1], Hilal A. Fadhil[2], Sinan Q. Salih[3], Taha A. Taha[4]

[1]Department of Medical Instrumentation Techniques Engineering, Technical Engineering College, Al-Kitab University, Kirkuk, Iraq
[2]Faculty of Electrical and Computer Engineering, Sohar University, Sohar, Oman
[3]Technical College of Engineering, Al-Bayan University, Baghdad, Iraq
[4]Unit of Renewable Energy, Northern Technical University, Kirkuk, Iraq

Article Info

ABSTRACT

This paper suggests a way of fixing problems of voltage fluctuations and peak overshoot in a PV-connected Zeta converter system. The Zeta converter in the proposed approach is controlled using proportional integral derivative (PID) while a genetic algorithm (GA) calculates the PID coefficients based on the control mechanism. The performance of the designed system was analyzed in a MATLAB/Simulink environment. The analysis showed that the proposed system reduced the output voltage ripple and peak overshoot during transient conditions by providing feedback to the converter through the PID controller, this is a significant improvement when compared to the results found without a PID controller.

Corresponding Author:

Abadal-Salam T. Hussain
Department of Medical Instrumentation Techniques Engineering, Technical Engineering College
Al-Kitab University
Altun Kupri, Kirkuk, Iraq
Email: asth2233@gmail.com

1. INTRODUCTION

Many nations are currently confronted with the challenge of meeting the rising power demand while having limited resources; as a result, researchers are exploring alternative methods of energy generation [1], [2]. Among these methods, DC-DC converters, also known as switching regulators, play a vital role in enhancing the efficiency of energy conversion in electric power extraction [3]. These converters facilitate the conversion of DC voltage to different levels while maintaining a stable output. They are commonly employed to obtain steady or adjustable DC voltages from a DC source. There are currently two major types of DC-DC converters - isolated converters and non-isolated converters; isolated converters, such as flyback and forward converters, incorporate a high-frequency transformer to ensure electrical isolation between the input and output (this offers protection to sensitive loads). However, this electrical isolation is not provided by non-isolated converters, such as buck, boost, buck-boost, design a single-ended primary-inductor converter (SEPIC), Cuk, and Zeta converters [4]–[7]. Compared to isolated converters, non-isolated converters are typically more affordable and easier to design. They are used in a variety of fields, including solar photovoltaic systems, distributed-DC systems, electric traction, specialized electrical machine drives, electric cars, distributed-DC systems, space applications, ships, and airplanes. To develop a highly effective system with outstanding power quality, the right DC-DC converter must be chosen because every application has unique needs.

The goals of this study are to develop a Zeta converter for photovoltaic (PV) applications with a variable input voltage and constant output voltage [8], create a "GA-optimized using proportional integral derivative (PID) controller for the Zeta converter [9], and evaluate the efficiency of the developed Zeta converter in terms of the voltage ripples and peak overshoot during transient" conditions. The basic concepts behind DC-DC conversion, in addition to a review of the earlier work in this field, were provided in this section of the paper. There are three major divisions in this section: i) The first part focused on the explanation of the popular converter types while; ii) The second part explored the existing zeta converter modeling strategies; and iii) The third part covered DC-DC converters using GA.

As seen in Figure 1, a power electronic converter consists of a power processor, a controller, and a voltage reference. The frequency, current, or voltage converter that makes up the power processor receives input power from the power source. The power is then converted by the power processor before being supplied to the load. Error minimization was ensured by comparing the "output voltage of the power processor (made up of the power electronic components) with the feedback voltage. The operation of both the switching and linear voltage regulators is reliant on this basic regulation" concept.
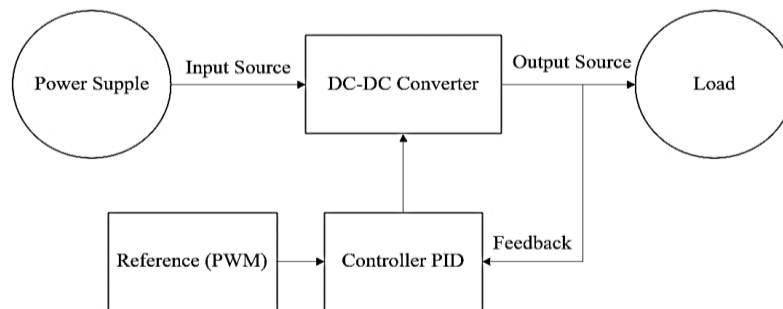

Figure 1. Block diagram DC-DC converter

2. ZETA CONVERTER

In various applications, an unregulated DC voltage, obtained by rectifying the mains voltage (as depicted in Figure 2), is commonly used as the input for converters. However, this input voltage tends to fluctuate due to variations in the line voltage magnitude. To ensure a constant and stable voltage, switch-mode DC-DC converters are employed; these converters take the unregulated input DC voltage and convert it to a fixed output voltage at the desired level. "With the use of switch-mode DC-DC converters, the fluctuations in the input voltage can be effectively regulated, providing a stable and reliable power source for applications involving DC motor drives and switch-mode DC voltage." The role of DC-DC converters in the control of switch-mode DC voltage and DC motor drive applications is significant [10]–[12]. A PV module and zeta converter is illustrated in the block diagram in Figure 3 [13].
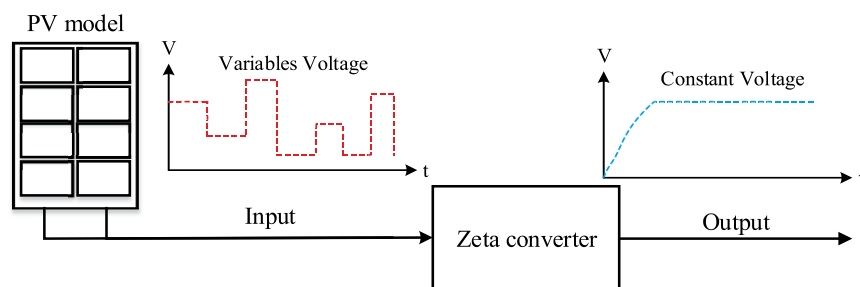

Figure 2. Block diagram for a PV module and a zeta converter

2.1. Continuous conduction mode (CCM) zeta converter

The zeta converter, which works in continuous conduction mode (CCM) [14], utilizes a switch (such as MOSFET or BJT) to control its operation. When the switch changes state, the diode also adjusts its state accordingly, either turning on or off (this configuration is illustrated in Figure 3). To minimize the ripple in the input current, two inductors (L1 and L2) are incorporated into the zeta converter. These inductors help smooth out the flow of current. Additionally, the circuit includes two capacitors (C1 and C2), with the assumption that these capacitors have sufficiently large values. Furthermore, the voltage across capacitor C2,

referred to as Vout, is maintained at a constant level. In summary, the zeta converter in continuous conduction mode utilizes a combination of a switch and diode, along with inductors and capacitors, to regulate the current and voltage in the circuit, ensuring stable operation and reduced ripple.
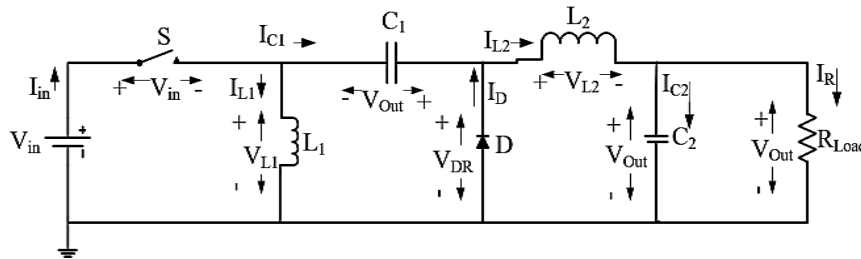

Figure 3. Circuit of the zeta DC-DC converter

2.2. Zeta converter control strat

The designed PID control system was implemented to regulate and control the operation of the zeta converter. This control system incorporates a feedback loop, allowing it to continuously monitor the output of the system and make necessary adjustments. The controller within the PID control system dynamically modifies the process based on the desired requirements. It actively adjusts various parameters to ensure that the zeta converter operates according to the desired specifications. By utilizing the feedback loop and implementing corrective measures, the PID control system maintains control over the zeta converter, enabling it to achieve the desired performance and effectively respond to system changes.

2.3. PID controller

The PID controller is employed to regulate "the varying input voltage of the zeta converter and ensure a stable output DC voltage level. The block diagram of the PID controller is presented in Figure 4. The PID controller utilizes feedback loops and aims to minimize the deviations between the desired set point and the calculated process values [15]–[20]. By adjusting the system parameters, the controller takes corrective actions to bring the process in line with the specified requirements. The PID controller configuration involves three essential variables: proportional (P), integral (I), and derivative (D). The proportional value (P) responds to the current error, the integral (I) considers the accumulated sum of past errors, and the derivative (D) takes into account the rate of change of the error. These variables are weighted and combined to modify the system behavior during the tuning process, allowing the PID controller to adapt to specific conditions and provide effective control actions. The converter is modeled using state space analysis (SSA) to ensure accurate determination of the state variables such as inductor current and capacitor voltage necessary for achieving a stable output voltage. The PID parameters are tuned based on delay time, rise time, peak time, & settling time. The optimal coefficients of the PID controller were calculated using Genetic algorithms (GA) to enable the automatic control features based on the PID controller with SSA". It is important to note that the utilization of the GA method for tuning the plant allows for optimization, resulting in suitable PID parameters that effectively regulate the system.
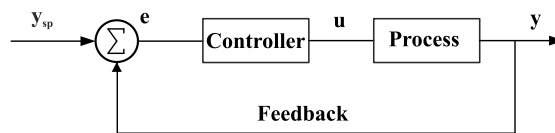

Figure 4. General block diagram for PID controller

2.4. Optimization of PID controller using genetic algorithm

GA is a comprehensive search method based on the principles of natural selection and mimics the process of evolution. It has demonstrated effectiveness in discovering superior solutions in complex domains, overcoming the problems of false optima and high dimensionality mostly associated with other gradient-descent methods. GA is, therefore, used in this study for the tuning of the controller via the provision of the optimal control parameters for the evaluation of the system performance. The GA follows specific steps to determine the optimal values of Kp, Ki, and Kd.

The fitness function in GA is used to evaluate the performance of individuals in the problem domain. In this particular problem, fitness is determined by the individual with the lowest numerical value associated with the objective function. The computation of fitness is commonly used to obtain performance metrics for each individual at intermediate stages [21]–[25]. The fitness function converts the objective function value into relative fitness measures. The objective function (f) is transformed (g) to non-negative numbers, and the obtained relative fitness (F) is used for filtering individuals and determining the expected offspring to be generated in the next generation.

Designing appropriate objective functions is the most challenging task in this project; the objective functions are essential for obtaining the optimal PID controller parameters that provide the fastest rise time and the least overshoot. In (1) serves as the objective function to evaluate the fitness of each chromosome.

$$MSE = \frac{1}{t}\int_0^\tau (e(t))^2\, dt, ITAE = \int_0^\tau t|e(t)|dt, IAE = \int_0^\tau |e(t)|dt, ISE = \int_0^\tau e(t)^2, ITSE = \int_0^\tau te(t)^2 dt \qquad (1)$$

The representation of the error signal in the time domain is given as e(t); in (1) comprises of the performance indices, such as "the mean square error (MSE)," "integral of time multiplied by absolute error (ITAE)," "integral of absolute magnitude of the error (IAE)," and "integral of square error (ISE)." This work proposed an objective function for the combination of these objective indices and the reduction of the error of the entire control system. The objective function, rather than performing a separate evaluation of each chromosome in the population, consider the entire control system at once. The evaluated chromosome is assigned a fitness number, where a higher number indicates better fitness. GA relies on the chromosomes with the fittest numbers to create a new population. This process continues until a final solution is obtained with a minimum percentage error. The PID controller is utilized to minimize the error signal, while the fitness of the chromosomes is determined by in (2).

$$Fitness\ value = \frac{1}{Performance\ index} \qquad (2)$$

2.5. Parameter calculation of zeta converter

The zeta converter system is designed to operate with an input voltage sourced from a PV module, which typically yields a variable voltage output of 38 V. The zeta converter's primary objective is to provide a stable DC output voltage of 13 V for various DC applications. To ensure the proper functioning of the system, certain limits and specifications are set. The current ripple across the inductors is limited to 0.15 A, while the ripple voltage across the capacitors is constrained to 1%. Additionally, the overshoot is restricted to a maximum of 1%. The zeta converter operates at a switching frequency (fsw) of 25 kHz, and it is subjected to a load of 10 Ω. By adhering to these specifications and considering the given operating conditions, the zeta converter system can effectively regulate the input voltage from the PV module and deliver a steady output voltage suitable for DC applications. The parameters of the designed zeta converter are given in Table 1.

Table 1. Parameters of the designed zeta converter

Parameters	Values	Parameters	Values
Input voltage, Vin	18 V	Ripple current inductor 2, ΔI (L2)	0.15 A
Output voltage, Vout	13 V	Inductor 2, L2	2 mH
Duty cycle, D	0.4194	Ripple voltage capacitor 1, ΔV (C1)	0.03 V
Frequency, f	25 kHz	Capacitor 1, C1	750 uF
Resistor, R	10 Ω	Ripple voltage capacitor 2, ΔV (C2)	0.03 V
Ripple current inductor 1, ΔI_{L1}	0.15 A	Capacitor 2, C2	25 uF

3.   SIMULATION RESULTS

The design of the zeta converter was implemented using MATLAB/Simulink. This involved obtaining the transfer function and performing state space analysis (SSA) for the zeta converter circuit. The stability of the system was assessed, leading to the design of a PID controller using the genetic algorithm (GA) for optimization. The performance of the transfer function was evaluated, and a Simulink model for the zeta converter was developed using the parameters listed in Table 1. Similarly, the parameters for the PID controller were selected from Table 1. The PID models were simulated, and the results were carefully documented. The genetic algorithm (GA) was employed to fine-tune the PID controller parameters and optimize performance according to the desired specifications. MATLAB/Simulink provided a comprehensive platform for the design process of the zeta converter model; it incorporates a PID controller and utilizes GA optimization to enhance system performance.

The PID controller was designed using GA as an optimizer for the determination of the optimal parameters. As a stochastic algorithm, GA mimics natural selection and serves as a global search method within GAs. It relies on the concepts of natural evolution for the exploration and identification of the most favorable parameter values for the PID controller.

3.1. Variable irradiances, constant temperature

The results obtained from the simulation study are highlighted in Table 2, the results showed that the irradiance kept increasing throughout the simulation. At the first stage of the simulation, the irradiance value was 0.4 kW/m^2 with a constant temperature of 25 °C and input voltage of 36.19 V. Similarly, the value of irradiance and input voltage kept increasing while the temperature remained constant at 25 °C. Nevertheless, the output voltage of the zeta converter remained constant at 13.01 V throughout the simulation irrespective of the change in irradiance and input voltage. In addition, the results also highlighted that increases in irradiance and input voltage only slightly increased the output voltage ripples. Furthermore, the peak overshoot values for each stage are also shown in Table 3, the results show that an increase in the irradiance value also increased the input voltage and the output voltage ripples. However, the highest peak overshoot value of 0.505% was obtained when the irradiance values were 0.8 kW/m^2 and 1.0 kW/m^2.

Table 2. Irradiance, temperature, input voltage, output voltage, output voltage ripple, and peak overshoot values obtained after simulation

Irradiance (W/m^2)	Temperature (°C)	Input voltage (V)	Output voltage (V)	Output voltage ripple	Peak overshoot (%)
400	25	36.19	13.01	9.85×10^{-2}	0.445%
600	25	36.88	13.01	1.00×10^{-1}	0.474%
800	25	37.34	13.01	1.02×10^{-1}	0.505%
1000	25	37.7	13.01	1.02×10^{-1}	0.505%

Table 3. Irradiance, temperature, input voltage, output voltage, output voltage ripple, and peak overshoot values obtained after simulation

Irradiance (W/m^2)	Temperature (°C)	Input voltage (V)	Output voltage (V)	Output voltage ripple	Peak overshoot (%)
400	25	36.19	13.01	9.85×10^{-2}	0.445%
600	25	36.88	13.01	1.00×10^{-1}	0.474%
800	25	37.34	13.01	1.02×10^{-1}	0.505%
1000	25	37.7	13.01	1.02×10^{-1}	0.505%

Figure 5 showed the simulation results of variations over time in values of irradiance and input voltage with constant temperature. During the first test, the irradiance was 0.4 kW/m^2 while the input voltage kept increasing towards 36.19 V. Similarly, at the maximum irradiance value of 1.0 kW/m^2, the maximum obtained value of input voltage was 37.7 V. Figure 6 showed the simulation results at multiple irradiance values of 0.4 kW/m^2, 0.6 kW/m^2, 0.8 kW/m^2, and 1.0 kW/m^2. Figure 6 also highlighted that with increases in irradiance, the input voltage values also kept increasing while the temperature remained constant. However, the zeta converter provided a constant output voltage of 13.01 V throughout the simulation irrespective of the changes in irradiance and input voltage values. The simulation results of the output voltage ripples for variable irradiance values at 0.4 kW/m^2, 0.6 kW/m^2, 0.8 kW/m^2, and 1.0 kW/m^2 are shown in Figure 7 along with varying input voltage values and constant temperature. As highlighted in Figure 7, the output voltage ripples change correspondingly with the change in irradiance; for instance, at the irradiance value of 0.4 kW/m^2, the output voltage ripple value was 9.85×10^{-2}. Furthermore, at the irradiance value of 0.6 kW/m^2, the output voltage ripple value was 1×10^{-1} and at the irradiance value of 0.8 W/m^2, the output voltage ripple value was 1.02×10^{-1}. Finally, the output voltage ripple value remained 1.02×10^{-1} at the irradiance value of 1.0 kW/m^2.

3.2. Variable irradiances, constant temperature

Table 4 showed the results of simulations in which the irradiance values were kept constant while the temperature was increasing. During the simulation of test 1, the value of irradiance was 1000 W/m^2 with a temperature of 25 °C at an input voltage of 37.7 V, the obtained output voltage from the zeta converter was constant at 13.01 V. Similarly, the value of temperature kept increasing and the input voltage value kept decreasing while the irradiance remained constant at 1000 W/m^2. Nevertheless, the output voltage of the zeta converter remained constant at 13.01 V throughout the simulation irrespective of the change in temperature and input voltage. Additionally, the results also highlighted that with temperature increases and decreases in input voltage, the output voltage ripples increased slightly. The peak overshoot values for each stage were also shown in Table 4.
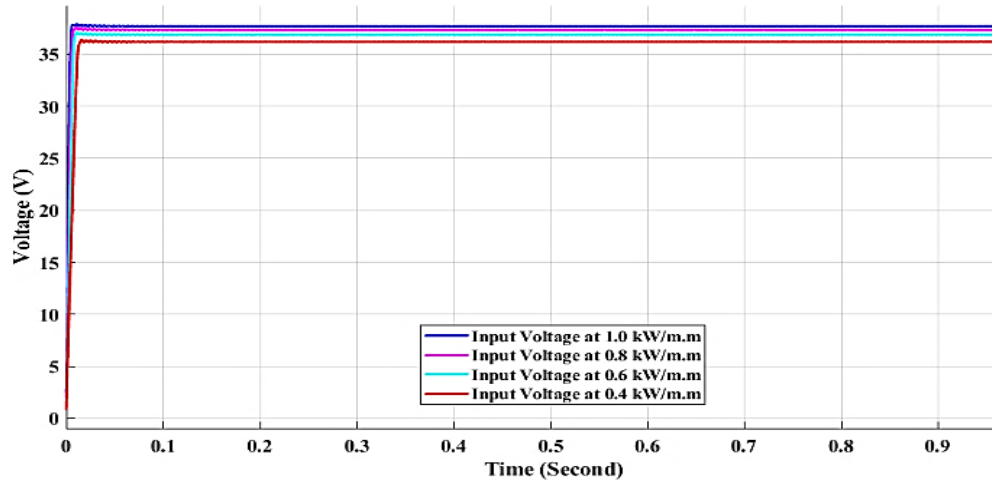
Figure 5. Variable irradiance and variable input voltage values at a constant temperature
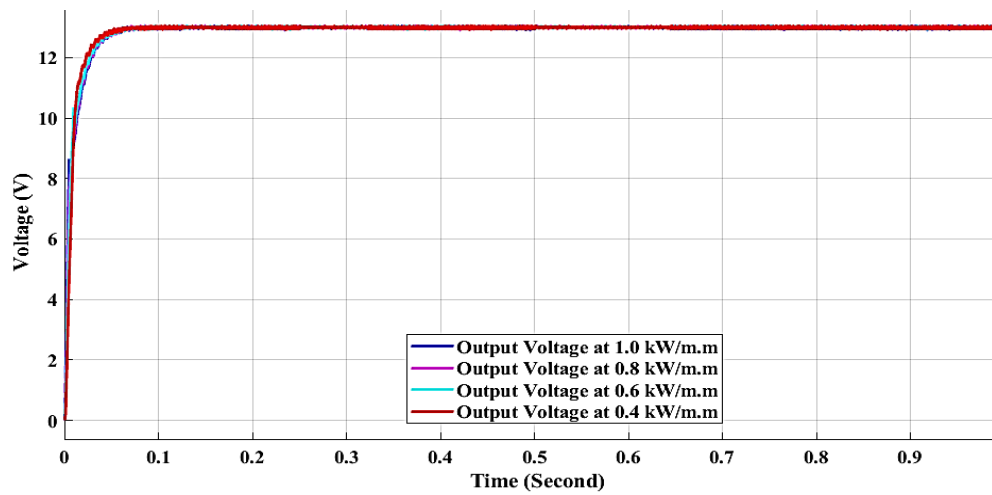

Figure 6. Constant output voltage irrespective of the variations in input voltage
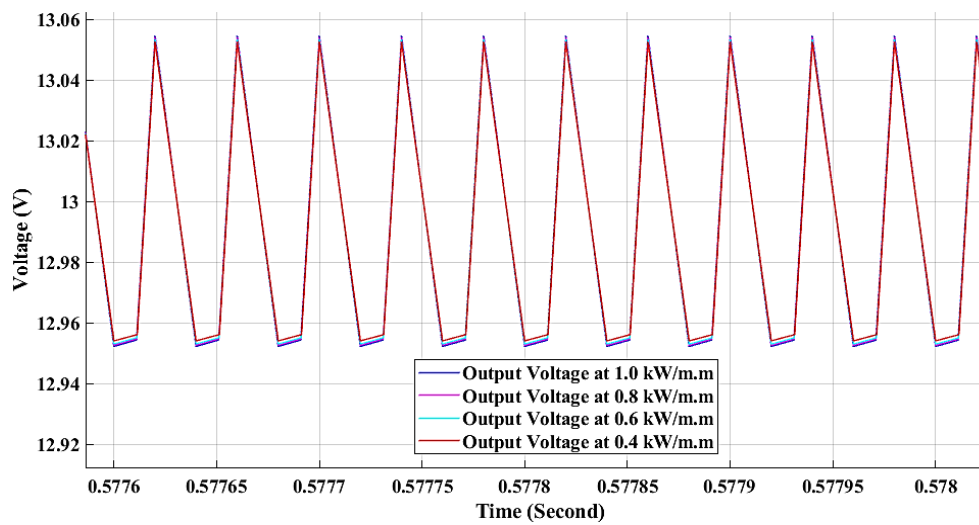

Figure 7. Output voltage ripples for variable irradiance

Table 4. Values of constant irradiance, varying temperature, input voltage, output voltage with small ripple and peak overshoot

Irradiance (W/m²)	Temperature (°C)	Input voltage (V)	Output voltage (V)	Output voltage ripple	Peak overshoot
1000	25	37.7	13.01	$1.02{\times}10^{-1}$	0.505%
1000	30	37.11	13.01	$1.01{\times}10^{-1}$	0.505%
1000	35	36.51	13.01	$9.93{\times}10^{-2}$	0.480%
1000	40	35.91	13.01	$9.77{\times}10^{-2}$	0.457%

Figure 8 showed the simulation results at a constant irradiance value and increasing temperature over time. The results also highlighted that during the test, temperature increases caused constant declines in the input voltage until the minimum value of 35.91 V. Figure 9 showed the result of the simulation where the irradiance value was kept constant at 1000 W/m² while the input voltage kept decreasing and the temperature kept increasing, the output provided by the zeta converter in this configuration remained constant at 13.01 V. Figure 10 showed the simulation results of output voltage ripples at a constant irradiance of 1000 W/m² and variable input voltage with varying temperature. At 25 °C and 30 °C temperatures, the values of the output voltage ripple were $1.02{\times}10^{-1}$ and $1.01{\times}10^{-1}$, respectively. Furthermore, the value of the output voltage ripple at the temperature of 35 °C was $9.93{\times}10^{-2}$ while at 40 °C, the output voltage ripple value was $9.7{\times}10^{-2}$.
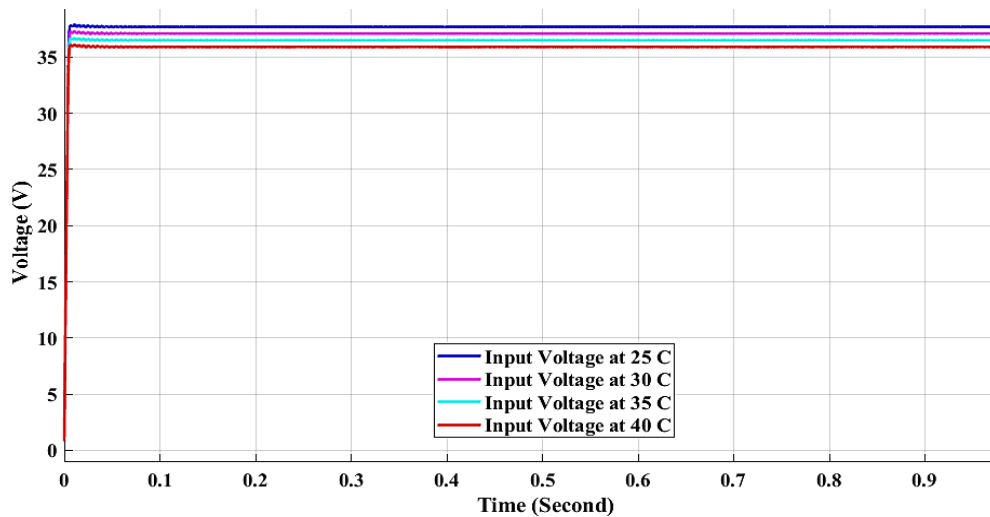

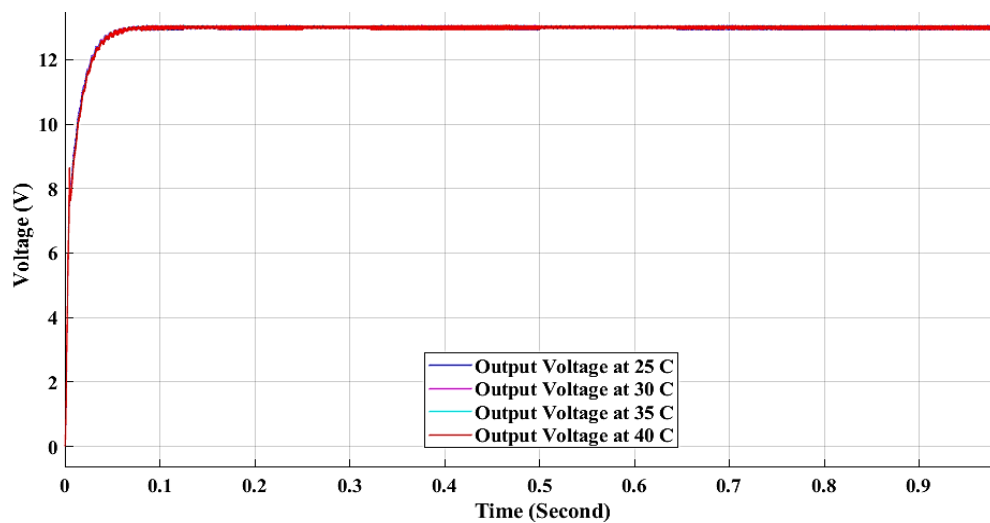Figure 8. Variable temperature and variable input voltage at constant irradiance

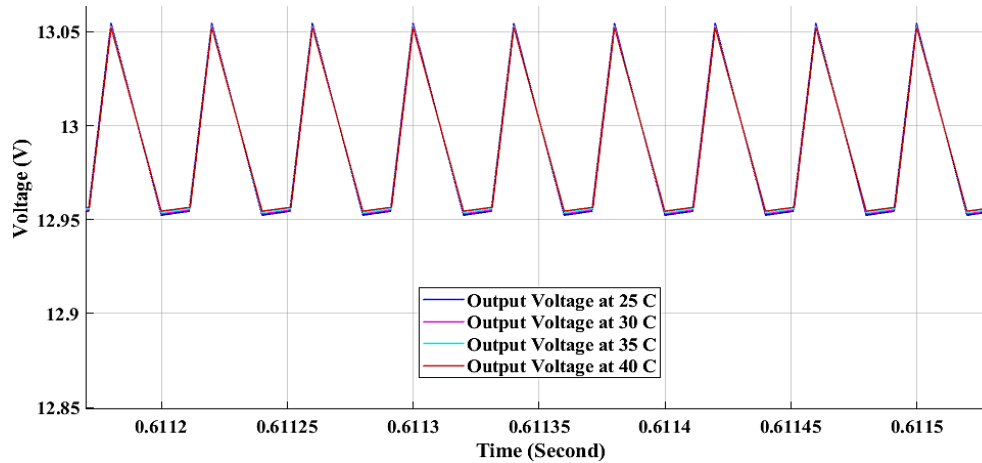Figure 9. Constant output voltage irrespective of the variations in input voltage

Figure 10. Output voltage ripples at variable temperature

3.3. Zeta variables of input voltage and constant output voltage

The simulation was conducted in MATLAB, as depicted in Figure 11, to observe the effect of varying the system's input voltage over time. It was observed that when the input voltage values were set at 31.56 V, 34.32 V, and 36.27 V, the output voltage remained constant at 13.01 V. Initially, starting with an input voltage of 34.32 V as the first step in the simulation, the output voltage consistently remained at 13.01 V over time. As the input voltage gradually increased, reaching 34.32 V at 0.329 seconds, the output voltage remained constant at 13.01 V. Subsequently, the input voltage continued to increase until it reached 36.27 V at 0.620 seconds, while the output voltage remained constant at 13.01 V. Overall, a constant output voltage of 13.01 V was maintained while the input voltages varied from 31.56 V to 36.27 V over time.
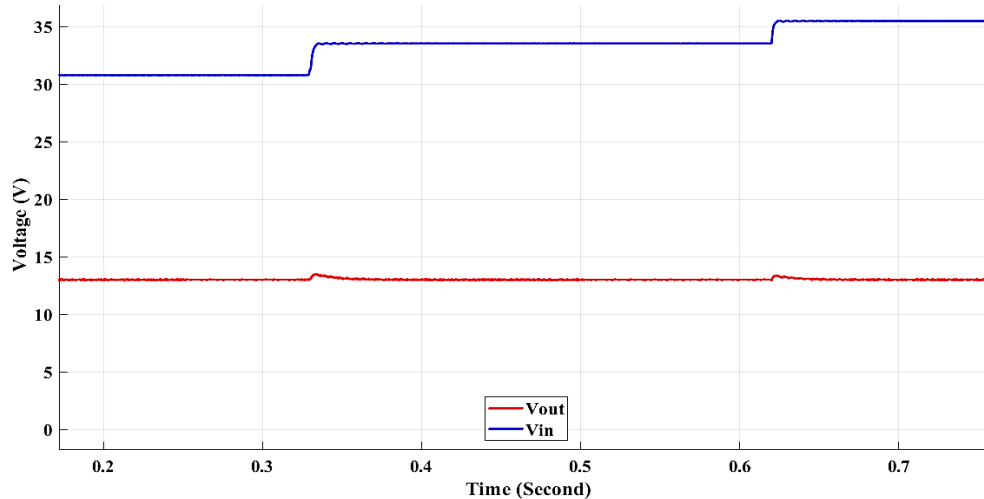
Figure 11. Increasing variable input voltages (31.56 V, 34.32 V, and 36.27 V) and steady output voltage (13.01 V)

Similarly, another simulation was conducted in MATLAB to examine the effect of decreasing the input voltage over time, as shown in Figure 11. When the initial step point was set at the maximum input voltage of 36.27 V, the output voltage remained constant at 13.01 V throughout the simulation. As the input voltage gradually decreased, reaching 34.32 V, the system continued to provide a constant output voltage of 13.01 V; it reached the minimum value of 31.56 V with a further decrease of the input voltage while the system maintained a constant output voltage of 13.01 V. In summary, Figure 11 demonstrates that a constant output voltage of 13.01 V was achieved while the input voltages varied from 36.27 V to 31.56 V over time.

Lastly, in Figure 12, the MATLAB simulation showed information regarding the system's performance when the input voltage is varied to different points (for instance, 31.56 V, 34.32 V, 36.27 V,

34.32 V, and 31.56 V) while still providing the constant output voltage of 13.01 V over time. At 31.56 V as the first step point in the simulation, the output voltage showed a constant output voltage of 13.01 V over time; the input voltage kept increasing after that until it reached 34.32 V at 0.172 seconds (the output voltage remained constant at 13.01 V). Later, the input voltage value was increased until it reached 36.27 V at 0.339 seconds and the output voltage remained at 13.01 V. The input voltage value was later increased to 34.32 V at 0.649 seconds and the output voltage remained constant at 13.01 V. Finally, the simulation results showed that the input voltage decreased from 34.32 V to 31.56 V at 0.801 seconds and the output voltage remained constant at 13.01 V as seen in Figure 13.
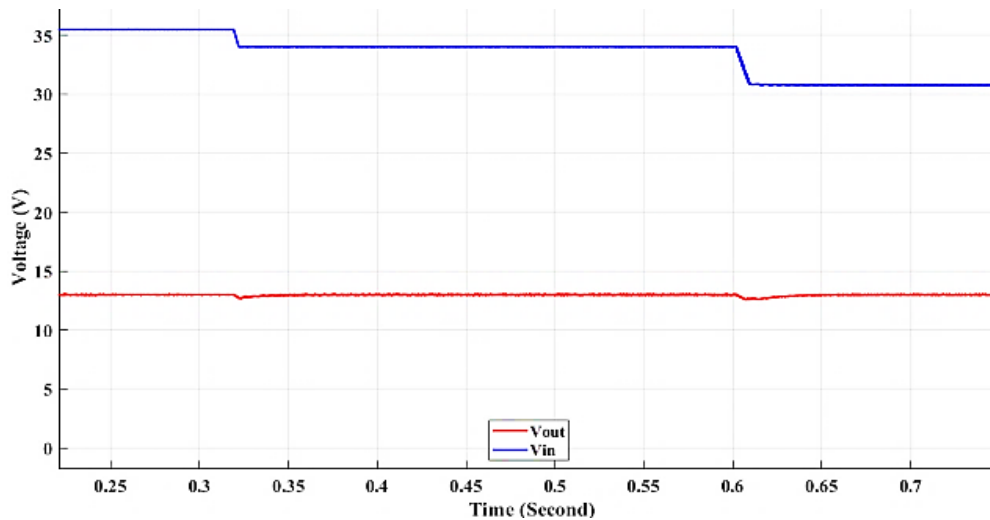
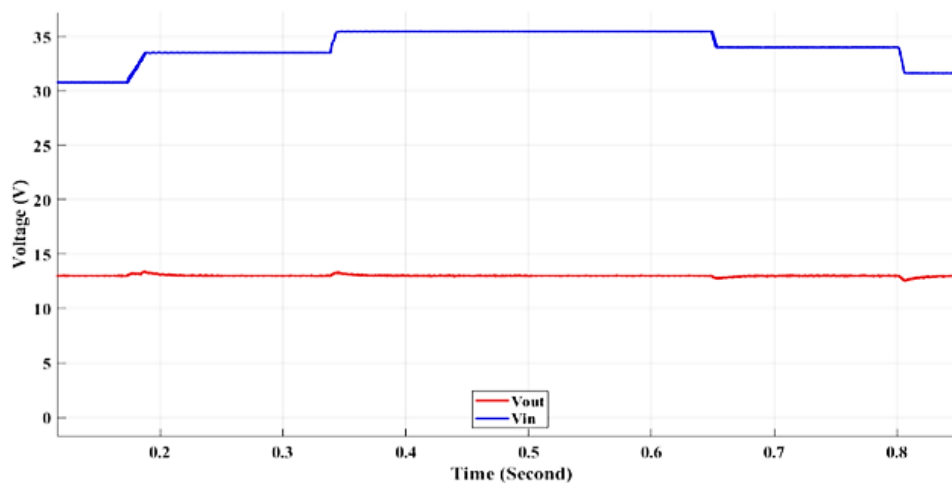Figure 12. Decreasing variable input voltages (36.27 V, 34.32 V, and 31.56 V) and stable output voltage (13.01 V)

Figure 13. Variable input voltages (31.56 V, 34.32 V, 36.27 V, 34.32 V, and 31.56 V) and stable output voltage (13.01 V)

4. CONCLUSION

The current study presents a solution to the issues of voltage ripple and peak overshoot during transient conditions. To achieve this, a genetic algorithm-based control mechanism was developed for the zeta converter to optimize the PID coefficients. The implementation of the zeta converter in continuous conduction mode and the performance analysis was conducted using MATLAB. The results obtained from the analysis demonstrate the effectiveness of the proposed system in reducing output voltage ripple and peak overshoot during transient conditions. A significant improvement was observed using the proposed solution

in comparison to the results obtained without the PID controller. Moreover, the zeta converter maintained a constant output voltage of 13 V throughout the entire duration regardless of variations in the input voltage from the PV module and different load conditions. The tests were performed under fixed changes in the irradiance and temperature of the zeta converter.

REFERENCES

[1]   P. Rathod, S. K. Mishra, and S. K. Bhuyan, "Renewable energy generation system connected to micro grid and analysis of energy management: A critical review," *International Journal of Power Electronics and Drive Systems*, vol. 13, no. 1, pp. 470–479, 2022, doi: 10.11591/ijpeds.v13.i1.pp470-479.

[2]   E. Jarmouni, A. Mouhsen, M. Lamhammedi, and H. Ouldzira, "Energy management system and supervision in a micro-grid using artificial neural network technique," *International Journal of Power Electronics and Drive Systems (IJPEDS)*, vol. 12, no. 4, p. 2570, Dec. 2021, doi: 10.11591/ijpeds.v12.i4.pp2570-2579.

[3]   A. K and S. K. S, "Closed loop control of DC-DC converters using PID and FOPID controllers," *International Journal of Power Electronics and Drive Systems (IJPEDS)*, vol. 11, no. 3, p. 1323, Sep. 2020, doi: 10.11591/ijpeds.v11.i3.pp1323-1332.

[4]   E. Bektaş and A. Karaarslan, "The comparison of PI control method and one cycle control method for SEPIC converter," *2017 10th International Conference on Electrical and Electronics Engineering, ELECO 2017*, vol. 2018-Janua, pp. 345–349, 2018.

[5]   M. Z. Zulkifli, M. Azri, A. Alias, M. H. N. Talib, and J. M. Lazi, "Simple control scheme buck-boost DC-DC converter for stand alone PV application system," *International Journal of Power Electronics and Drive Systems (IJPEDS)*, vol. 10, no. 2, p. 1090, Jun. 2019, doi: 10.11591/ijpeds.v10.i2.pp1090-1101.

[6]   W. M. Utomo *et al.*, "Voltage tracking of bridgeless PFC cuk converter using PI controller," *International Journal of Power Electronics and Drive Systems (IJPEDS)*, vol. 11, no. 1, p. 367, Mar. 2020, doi: 10.11591/ijpeds.v11.i1.pp367-373.

[7]   N. Siddharthan and B. Balasubramanian, "Performance evaluation of SEPIC, Luo and ZETA converter," *International Journal of Power Electronics and Drive Systems (IJPEDS)*, vol. 10, no. 1, p. 374, Mar. 2019, doi: 10.11591/ijpeds.v10.i1.pp374-380.

[8]   W. Abitha Memala, C. Bhuvaneswari, S. M. Shyni, G. Merlin Sheeba, M. S. Mahendra, and V. Jaishree, "DC-DC converter based power management for go green applications," *International Journal of Power Electronics and Drive Systems*, vol. 10, no. 4, pp. 2046–2054, 2019, doi: 10.11591/ijpeds.v10.i4.pp2046-2054.

[9]   K. Andal C. and J. R., "Improved GA based power and cost management system in a grid-associated PV-wind system," *International Journal of Power Electronics and Drive Systems (IJPEDS)*, vol. 12, no. 4, p. 2531, Dec. 2021, doi: 10.11591/ijpeds.v12.i4.pp2531-2544.

[10]   M. Forouzesh, Y. P. Siwakoti, S. A. Gorji, F. Blaabjerg, and B. Lehman, "Step-Up DC-DC converters: A comprehensive review of voltage-boosting techniques, topologies, and applications," *IEEE Transactions on Power Electronics*, vol. 32, no. 12, pp. 9143–9178, 2017, doi: 10.1109/TPEL.2017.2652318.

[11]   J. Falin, "Designing DC/DC Converters based on ZETA Topology," *Analog Applications Journal Texas Instruments Incorporated*, vol. 2Q, pp. 16–21, 2010.

[12]   E. Vuthchhay, C. Bunlaksananusorn, and H. Hirata, "Dynamic Modeling and Control of a Zeta Converter," in *2008 International Symposium on Communications and Information Technologies*, Oct. 2008, pp. 498–503. doi: 10.1109/ISCIT.2008.4700242.

[13]   S. Semeskandeh, M. Hojjat, and M. H. Abardeh, "Design of a photovoltaic mppt charge controller using DC-DC zeta converter with a modified three-stage charging method," *International Journal of Power Electronics and Drive Systems (IJPEDS)*, vol. 13, no. 3, p. 1887, Sep. 2022, doi: 10.11591/ijpeds.v13.i3.pp1887-1894.

[14]   M. Mahdavi and H. Farzanehfard, "Bridgeless SEPIC PFC Rectifier With Reduced Components and Conduction Losses," *IEEE Transactions on Industrial Electronics*, vol. 58, no. 9, pp. 4153–4160, Sep. 2011, doi: 10.1109/TIE.2010.2095393.

[15]   M. M. Nishat, F. Faisal, A. J. Evan, M. M. Rahaman, M. S. Sifat, and H. M. F. Rabbi, "Development of Genetic Algorithm (GA) Based Optimized PID Controller for Stability Analysis of DC-DC Buck Converter," *Journal of Power and Energy Engineering*, vol. 08, no. 09, pp. 8–19, 2020, doi: 10.4236/jpee.2020.89002.

[16]   M. M. Nishat, F. Faisal, and M. A. Hoque, "Modeling and Stability Analysis of a DC-DC SEPIC Converter by Employing Optimized PID Controller Using Genetic Algorithm," *International Journal of Electrical & Computer Sciences IJECS-IJENS*, vol. 19, no. 01, pp. 1–7, 2019.

[17]   B. Pid, D. S. Converter, M. M. Nishat, F. Faisal, A. Hoque, and A. J. Evan, "Stability Analysis and Optimization of Simulated Annealing (SA) Algorithm Stability Analysis and Optimization of Simulated Annealing (SA) Algorithm Based PID Controller for DC-DC SEPIC Converter," no. September, 2019.

[18]   M. M. Nishat, F. Faisal, M. Rahman, and M. A. Hoque, "Modeling and Design of a Fuzzy Logic Based PID Controller for DC Motor Speed Control in Different Loading Condition for Enhanced Performance," in *2019 1st International Conference on Advances in Science, Engineering and Robotics Technology (ICASERT)*, May 2019, pp. 1–6. doi: 10.1109/ICASERT.2019.8934559.

[19]   E. Kumru and N. F. O. Serteller, "DC motor Analysis Based on Improvement of PID Coefficients Using PSO Algorithm for Educational Use," *Lecture Notes in Networks and Systems*, vol. 633 LNNS, pp. 901–909, 2023, doi: 10.1007/978-3-031-26876-2_85.

[20]   J. Han, X. Shan, H. Liu, J. Xiao, and T. Huang, "Fuzzy gain scheduling PID control of a hybrid robot based on dynamic characteristics," *Mechanism and Machine Theory*, vol. 184, p. 105283, Jun. 2023, doi: 10.1016/j.mechmachtheory.2023.105283.

[21]   E. Bektas and H. Karaca, "GA Based Selective Harmonic Elimination for Five-Level Inverter Using Cascaded H-bridge Modules," *International Journal of Intelligent Systems and Applications in Engineering*, vol. 4, no. 2, p. 29, 2016, doi: 10.18201/ijisae.97681.

[22]   A. Lambora, K. Gupta, and K. Chopra, "Genetic Algorithm- A Literature Review," in *2019 International Conference on Machine Learning, Big Data, Cloud and Parallel Computing (COMITCon)*, Feb. 2019, pp. 380–384. doi: 10.1109/COMITCon.2019.8862255.

[23]   H. Wang *et al.*, "Multi-objective optimization of a hydrogen-fueled Wankel rotary engine based on machine learning and genetic algorithm," *Energy*, vol. 263, p. 125961, Jan. 2023, doi: 10.1016/j.energy.2022.125961.

[24]   G. Papazoglou and P. Biskas, "Review and Comparison of Genetic Algorithm and Particle Swarm Optimization in the Optimal Power Flow Problem," *Energies*, vol. 16, no. 3, p. 1152, Jan. 2023, doi: 10.3390/en16031152.

[25]   E. Bektas and H. Karaca, "GA based selective harmonic elimination for multilevel inverter with reduced number of switches: An experimental study," *Elektronika ir Elektrotechnika*, vol. 25, no. 3, pp. 10–17, 2019, doi: 10.5755/j01.eie.25.3.23670.

BIOGRAPHIES OF AUTHORS

Abadal-Salam T. Hussain ⓘ 🄶 sc ⊙ is currently a Ph.D. faculty staff, Assistant Professor– Department head of Medical Instrumentations Technique Engineering, Alkitab University. Previously faculty staff of School of Electrical System Engineering, University Malaysia Perlis (UniMAP), Malaysia (2013-2016). He also has a GCE from the University of London & a Bachelor of Engineering from the Royal Naval Engineering College, Manadon, Plymouth, UK in 1989. He also has a Master of Science awarded by the University of Science & Technology Oran Algeria in 2000 and a doctorate (PhD) in Mechatronic Engineering awarded by the University Malaysia Perlis (UniMAP) in 2013. He can be contacted at email: asth2233@gmail.com, or asth3@yahoo.com.

Faris Hassan Taha ⓘ 🄶 sc ⊙ is currently a Ph.D. faculty staff, Assistant Professor– Department of Medical Instrumentations Technique Engineering, Al-Kitab University. Previously University of Mosul staff at Department of Electrical Engineering, (2006-2020). He has got a Bachelor of Engineering (B.Sc.) from Department of Electrical, University of Mosul. He also has awarded a master of science (M.Sc.) by the University of Mosul Electronic and Communications. He also awarded a Doctorate of Philosophy (PhD) in Solid State Electronics and Microelectronics in 2013 from Department of Electrical, University of Mosul. He can be contacted at email: en.fa.aldabbagh@gmail.com, or f.h.aldabbagh@uomosul.edu.iq.

Hilal A. Fadhil ⓘ 🄶 sc ⊙ is Ph.D. in Telecommunication Engineering. He is currently an assist professor at sohar University. His research interests include Free-space optic, Optical CDMA, LiFi technologies and wavelength division multiplexing for Optical Access Networks. He holds several copyrights, patents in the UK and Malaysia and published more than 100 reviewed conference papers and indexed journal articles (citation 1882; H-index 18; RG: 27.97). Owing to his many research and product achievements and contributions, Hilal A. Fadhil was awarded many Awards and Medals in UK, Germany, South Korea and Malaysia; He is a senior member of IEEE communication (MIEEE-USA); Member of the Institution of Engineering & Technology (MIET-UK), and Optical Society of America (SPIE). He is also an editor for IEEE Communications Magazine, Optical Engineering Society, IET Optoelectronics and the founding Reviewer of the IEEE communication letter. He can be contacted at email: Dr.hilal.adnan@gmail.com.

Sinan Q. Salih ⓘ 🄶 sc ⊙ received the B.Sc. degree in information systems from the University of Anbar, in 2010, the M.Sc. degree in computer science from the College of Information Technology, University Tenaga Nasional (UNITEN), in 2012, and the Ph.D. degree in soft computing and intelligent systems from the Faculty of Software Engineering, University of Malaysia Pahang (UMP), in 2019. He is currently a Lecturer with the Technical College of Engineering, Al-Bayan University. He published over 70 research papers, and coauthored with more than 50 researchers. His current research interests include optimization algorithms, nature-inspired metaheuristics, machine learning, and feature selection problem for real-world problems. He can be contacted at email: sinan.salih@albayan.edu.iq.

Taha A. Taha ⓘ 🄶 sc ⊙ is a recipient of a mixed-mode master's degree, M.Sc., in Electrical Power Engineering from the University Malaysia Perlis (UniMAP) (2019) in Malaysia. He also holds a Bachelor's degree from the School of Electrical System at the University Malaysia Perlis (UniMAP) (2017) and a diploma in IT skills from the University of Cambridge, UK (2012). He can be contacted at email: t360pi@gmail.com.